A&A 639, L5 (2020)
https://doi.org/10.1051/0004-6361/202038398

Astronomy & Astrophysics

LETTER TO THE EDITOR

Preflare very long-periodic pulsations observed in Hα emission before the onset of a solar flare*

Dong Li[1,2,3], Song Feng[4], Wei Su[5], and Yu Huang[1]

[1] Key Laboratory of Dark Matter and Space Astronomy, Purple Mountain Observatory, CAS, Nanjing 210033, PR China
e-mail: lidong@pmo.ac.cn
[2] State Key Laboratory of Space Weather, Chinese Academy of Sciences, Beijing 100190, PR China
[3] CAS Key Laboratory of Solar Activity, National Astronomical Observatories, Beijing 100101, PR China
[4] Yunnan Key Laboratory of Computer Technology Application, Faculty of Information Engineering and Automation, Kunming University of Science and Technology, Kunming 650500, PR China
[5] MOE Key Laboratory of Fundamental Physical Quantities Measurements, School of Physics, Huazhong University of Science and Technology, Wuhan 430074, PR China

Received 12 May 2020 / Accepted 23 June 2020

ABSTRACT

Context. Very long-periodic pulsations during preflare phases (preflare-VLPs) have been detected in the full-disk solar soft X-ray (SXR) flux. They may be regarded as precursors to solar flares and may help us better understand the trigger mechanism of solar flares.

Aims. In this Letter, we report a preflare-VLP event prior to the onset of an M1.1 circular-ribbon flare on 2015 October 16. It was simultaneously observed in Hα, SXR, and extreme ultraviolet (EUV) wavelengths.

Methods. The SXR fluxes in 1−8 Å and 1−70 Å were recorded by the Geostationary Operational Environmental Satellite (GOES) and Extreme Ultraviolet Variability Experiment, respectively; the light curves in Hα and EUV 211 Å were integrated over a small local region, which were measured by the 1 m New Vacuum Solar Telescope and the Atmospheric Imaging Assembly (AIA), respectively. The preflare-VLP is identified as the repeat and quasi-periodic pulses in light curves during preflare phase. The quasi-periodicity can be determined from the Fourier power spectrum with Markov chain Monte Carlo-based Bayesian.

Results. Seven well-developed pulses are found before the onset of an M1.1 circular-ribbon flare. They are firstly seen in the local light curve in Hα emission and then discovered in full-disk SXR fluxes in GOES 1−8 Å and ESP 1−70 Å, as well as the local light curve in AIA 211 Å. These well-developed pulses can be regarded as the preflare-VLP, which might be modulated by LRC-circuit oscillation in the current-carrying plasma loop. The quasi-period is estimated to be ~9.3 min.

Conclusions. We present the first report of a preflare-VLP event in the local Hα line and EUV wavelength, which could be considered a precursor of a solar flare. This finding should therefore prove useful for the prediction of solar flares, especially for powerful flares.

Key words. Sun: flares – Sun: oscillations – Sun: chromosphere – Sun: UV radiation – Sun: X-rays, gamma rays

1. Introduction

Solar flares represent the rapid and violent process of releasing magnetic free energy by reconnection, which is often characterized by a complex magnetic field (see Benz 2017, for a review). The coupling of a complex magnetic structure and plasma during a solar flare usually causes a quasi-periodic phenomenon, which is referred to as the quasi-periodic pulsation (QPP, see Nakariakov et al. 2019a; Kupriyanova et al. 2020, for recent reviews). It is a common oscillatory feature in the light curve of solar flare, which was first detected in X-ray and microwave emission (e.g., Parks & Winckler 1969) and later discovered in nearly all electromagnetic radiation, such as radio (Ning et al. 2005; Karlický et al. 2020), extreme-ultraviolet (EUV, Shen et al. 2019; Yuan et al. 2019), X-ray (Ning 2014; Dennis et al. 2017), and even γ-ray (Nakariakov et al. 2010; Li et al. 2020a). It could be observed in the preflare phase (e.g., Zhou et al. 2016; Li et al. 2020b), rising and postflare phases (Kolotkov et al. 2015; Li et al. 2017; Ning 2017; Hayes et al. 2019). The detected periods in solar flares vary from subseconds to hundreds of seconds, which strongly depend on the observed instruments and wavelengths (e.g., Tan et al. 2007; Shen et al. 2013; Inglis et al. 2016; Li et al. 2016; Pugh et al. 2019; Yu & Chen 2019). The QPPs can be found in most flare events, however, their generation mechanisms are still highly debated (see Van Doorsselaere et al. 2016; McLaughlin et al. 2018, for reviews), which might be attributed to magnetohydrodynamic (MHD) waves (Anfinogentov et al. 2015; Wang et al. 2015; Tian et al. 2016; Nakariakov et al. 2019b) or repetitive magnetic reconnection (Kliem et al. 2000; Thurgood et al. 2017; Li et al. 2020c). Previous observations also found that the periods could depend on the mechanism producing them (e.g., Tan et al. 2010). The short periods, such as 10−100 s, detected in hard X-ray or γ-ray etc are usually associated with the nonthermal electrons or ions that have been accelerated by the repetitive reconnection (e.g., Aschwanden et al. 1995; Nakariakov et al. 2010;

* Movie is available at https://www.aanda.org

Li et al. 2020a). The long periods (i.e., 5−40 min), however, are often attributed to the MHD waves; for instance, the transverse oscillations observed in coronal loops, which were often interpreted as the kink-mode waves (e.g., Nakariakov et al. 1999; Duckenfield et al. 2019), as well as the standing slow-mode waves detected in hot (>6 MK) loops measured by the SUMER spectrometer, which were referred as SUMER oscillations (Wang et al. 2002, 2003; Wang 2011).

In recent years, the studies of flare-related QPPs have achieved significant progress in understanding the dynamic of solar flares, so they must be taken account when constructing the flare model (Kupriyanova et al. 2020). Moreover, the QPP has been observed during preflare phase, which could be regarded as the precursor of a solar flare, in other words, as a convenient precursory indicator for the powerful (M- or X-) flare (e.g, Tan et al. 2016; Zhou et al. 2016). Therefore, investigating QPPs before the onset of solar flares can help us to understand their trigger mechanism and origin source. Using soft X-ray (SXR) fluxes recorded by the Geostationary Operational Environmental Satellite (GOES), Tan et al. (2016) first reported the QPPs with typical periods of 8−30 min during preflare phases and they referred to them as very long pulsations in the preflare phase (preflare-VLPs). On the other hand, QPPs in Hα emissions have also been reported, such as sausage oscillations in the cool post-flare loop (e.g., Srivastava et al. 2008), and the multiple periodic oscillations in newly formed loops following small-scale magnetic reconnection (e.g., Yang & Xiang 2016). The detection of QPPs in Hα emissions could provide essential information for understanding MHD waves in the solar chromosphere (Jess et al. 2015). However, the preflare-VLPs in Hα emission are rarely reported. In this Letter, we investigate a preflare-VLP event in Hα, SXR and EUV wavebands. The preflare-VLP shares a same source with the accompanied M1.1 flare, implying it could be the precursor of the main flare. This Letter is organized as follows: Sect. 2 describes the observations and Sect. 3 presents our main results. The conclusion and discussion are summarized in Sect. 4.

2. Observations

On October 16, 2015, an M1.1 circular-ribbon flare took place in the active region (AR) NOAA 12434 (S11E45). The energy partition of this circular-ribbon flare has been studied in detail by Zhang et al. (2019). In this study, we focus on the preflare phase before the onset of the circular-ribbon flare, that is, between ~05:01 UT and ~06:10 UT. It was simultaneously observed by GOES, as well as the 1m New Vacuum Solar Telescope (NVST, Liu et al. 2014), Atmospheric Imaging Assembly (AIA, Lemen et al. 2012), and the Extreme Ultraviolet Variability Experiment (EVE, Woods et al. 2012) onboard the Solar Dynamics Observatory (SDO).

The NVST is a one meter aperture vacuum telescope located at Fuxian Solar Observatory, which is operated by Yunnan Observatory of the Chinese Academy of Sciences. It mainly provides high resolution images in Hα and TiO channels (Liu et al. 2014). In this study, Hα level1 data at the wavelength of 6562.8 Å between ~05:01 UT and ~06:10 UT were used to investigate the preflare-VLP. They were processed by the frame selection (lucky imaging) from a large number of short-exposure images (see Tubbs 2004; Liu et al. 2014; Xu et al. 2014; Xiang et al. 2016). The Hα images in the line center are used here, which have a spatial scale of ~0.16 pixel^{-1} and a time cadence of ~48 s. We also use the SXR fluxes recorded by GOES and the EUV SpectroPhotometer (ESP) for SDO/EVE, and the EUV image at AIA 211 Å.

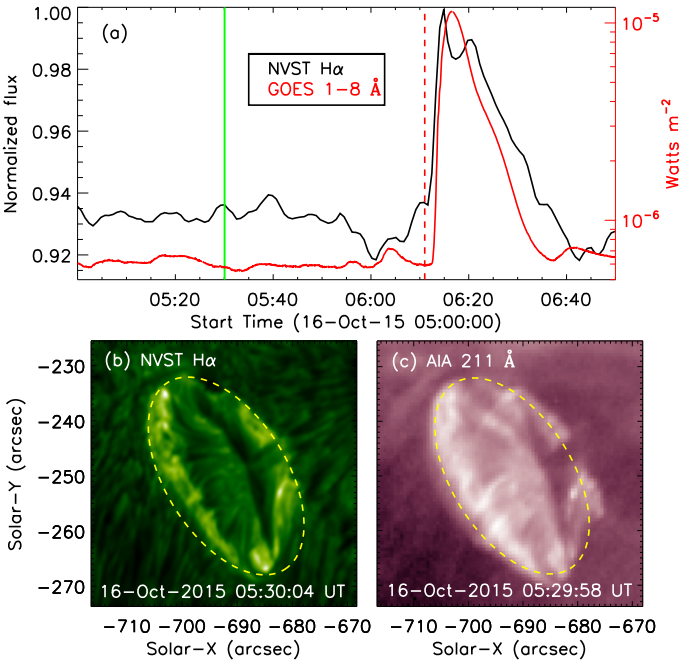

Fig. 1. *Panel a*: light curve integrated over a small local region (~48″ × 48″) in Hα line center (black) and the full-disk flux in SXR 1−8 Å (red) from 05:00 UT to 06:50 UT on 2015 October 16. The red vertical line indicates the onset of the M1.1 flare. *Panels b and c*: snapshots with a FOV of ~48″ × 48″ at wavelengths of Hα 6562.8 Å and AIA 211 Å at about 05:30 UT, as indicated by the green line in *panel a*. The yellow dashed line outlines an ellipse profile. The whole evolution is shown in the online video, anim.mp4.

Figure 1a presents the SXR flux in GOES 1−8 Å (red), which shows a swift enhancement at around 06:11 UT (red vertical line), suggesting an M1.1 flare erupts. Some small pulses before the onset of the M1.1 flare can be seen, which might be regarded as the preflare-VLP (e.g., Tan et al. 2016). We then plot the light curve in Hα emission integrated over a local region with a small field-of-view (FOV) of about 48″ × 48″, as shown with the black curve. We can find a series of pronounced pulses in the preflare phase. Panels b and c draw the local images at around 05:30 UT (green vertical line in panel a) in Hα and AIA 211 Å, respectively. They have the same FOV and display a circular profile, indicating a followed circular-ribbon flare (see, Zhang et al. 2019; Zhang & Zheng 2020). The whole evolution from ~05:01 UT to ~06:20 UT can be seen in the online video, anim.mp4.

3. Results

Taking a closer look at the small pulses in the preflare phase, Fig. 2 shows the local light curves during 05:01−06:10 UT in Hα (black) and AIA 211 Å (magenta), as well as the full-disk light curves in GOES 1−8 Å (red) and ESP 1−70 Å (cyan). All these light curves have been normalized and shifted in height so that they may be clearly shown in the same window. We can find seven well-developed pulses in the local Hα light curve, each of them assigned a number, and their peak times are marked by orange vertical lines. The pulse period is estimated to be in the range of 6−11.5 min, with an average periodicity of ~9.3 min. We also notice that the pulse period from peak "1" to peak "5" is roughly constant, but it changes clearly after peak "5". In the full-disk SXR fluxes at GOES 1−8 Å and ESP 1−70 Å, we can

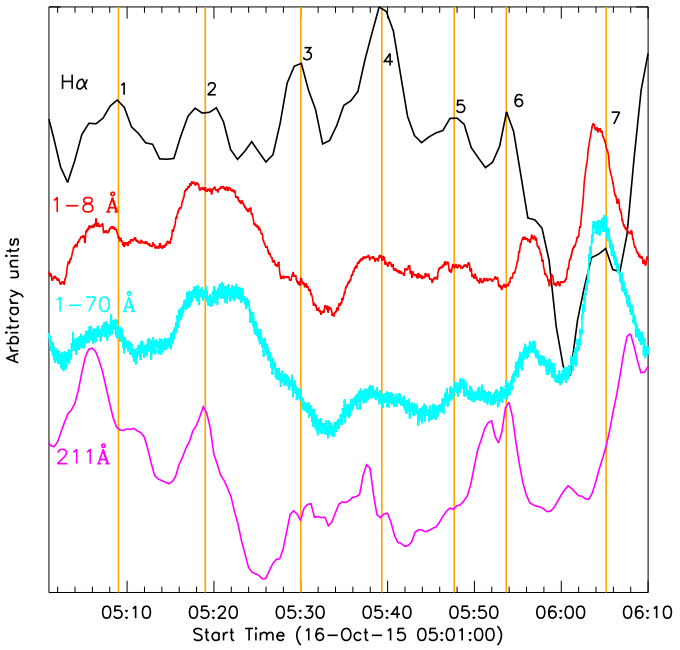

Fig. 2. Normalized light curves between 05:01 UT and 06:10 UT in Hα 6562.8 Å (black), GOES 1−8 Å (red), ESP 1−70 Å (cyan), and AIA 211 Å (magenta). The orange lines mark the pulsation peak time in the Hα light curve. We note that the light curves have been shifted in the y axis so they can clearly be shown in the same window.

find the seven pulses with the period that is similar to the Hα pulses. Moreover, the two SXR fluxes are almost in phase with each other. We also note that pulse "3" is weak at GOES 1−8 Å and it is hard to distinguish in ESP 1−70 Å. Then seven major pulses are identified in the local light curve at the wavelength of AIA 211 Å, with the similar period for these pulses in the Hα light curve.

To determine the time delay in different wavelengths, the cross-correlation analysis (Tian et al. 2012, 2016; Su et al. 2016, etc) is applied to these normalized light curves, as shown in Fig. 3. A maximum correlation coefficient of ∼0.5 can be found at the time lag of roughly 1.8 min (marked by a black arrow), suggesting a short time delay between the Hα light curve and the GOES 1−8 Å flux. The same time delay can be found between the Hα light curve and the ESP 1−70 Å flux (cyan), which also implies that the pulses in SXR fluxes recorded by GOES and EVE are fully in phase. We also find a maximum correlation coefficient of ∼0.66 at the time lag of roughly 4.5 min (marked by a magenta arrow), indicating a long time delay between the Hα light curve and the AIA 211 Å flux.

The pulse period is estimated by directly counting the pulses before the onset time of the M1.1 flare (Fig. 2), which is straightforward and quite simple (see, Tan et al. 2016). To examine their periodicity, we then perform a mathematical analytic method to the original light curves, that is, a fast Fourier transformation, as shown in Fig. 4. The red noise here is estimated with Multi-parameter Bayesian inferences based on Markov chain Monte Carlo (MCMC) samples (see, Liang et al. 2020). Panel a shows the Hα light curve during ∼05:01−06:10 UT and it has been normalized by $(I-\bar{I})/\bar{I}$, where I and $\bar{I}$ are the observational intensities and their average intensity, respectively. The power spectral density (PSD) of the normalized light curve are given in panel b, displayed in a log-log space. Based on this, a period of about 9.3 min is clearly found to be above the 95% confidence level

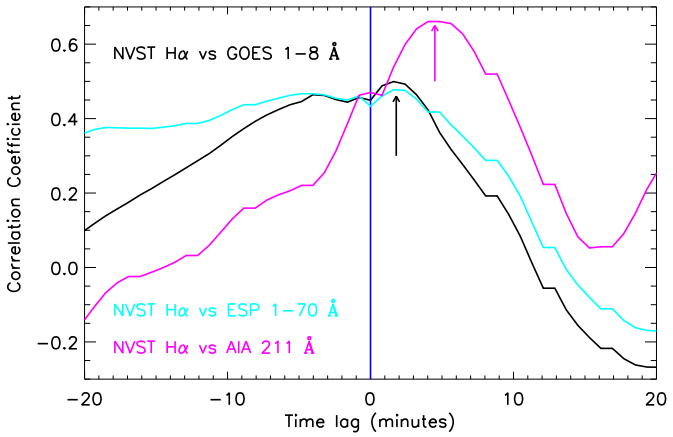

Fig. 3. Correlation coefficients between two light curves as a function of the time lag, such as NVST Hα and GOES 1−8 Å (black), ESP 1−70 Å (cyan), and AIA 211 Å (magenta). A blue vertical line indicates at the time lag of "0".

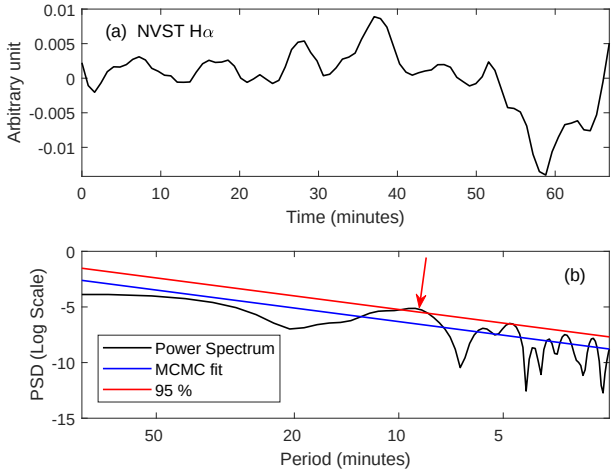

Fig. 4. Normalized Hα light curve (a) and its corresponding PSD (b) in log-log space. The blue line represents the best (MCMC) fit, while the red line indicates the 95% confidence level. The red arrow marks the period which is above the confidence level.

(red line), as indicated by a red arrow. The MCMC result is consistent with previous findings based on a direct count of the pulses.

4. Conclusions and discussion

Using the NVST data, a quasi-periodic pulsation event with a period of ∼9.3 min was discovered in Hα emission prior to the onset of an M1.1 circular-ribbon flare on 2016 October 16. A similar periodic pulsation is also detected in the full-disk SXR fluxes recorded by the GOES and the SDO/EVE, as well as the local EUV flux measured by the SDO/AIA. Based on the SXR emission observed by the GOES, the very long periodic pulsations prior to the onset of solar flares were reported by Tan et al. (2016) and referred to as preflare-VLPs. Here, the periodic pulsation event observed at the wavelengths of Hα 6562.8 Å, AIA 211 Å, GOES 1−8 Å and ESP 1−70 Å in the preflare phase could also be regarded as a preflare-VLP. Moreover, the Hα and AIA imaging observations suggest that the preflare-VLP shares a same source origin region with the accompanying circular-ribbon flare, further confirming that the

preflare-VLP ought to be considered a precursor of the main flare. Similar to the preflare coronal dimming (Zhang et al. 2017) and the chromospheric evaporation in flare precursor (Li et al. 2018), the preflare-VLP cold be used to predict a solar flare; in particular, it can be regarded as a precursory indicator for the powerful flare (Tan et al. 2016; Zhou et al. 2016).

It is very interesting to note that a preflare-VLP has been simultaneously observed in the Hα, SXR, and EUV wavebands. The detected period is similar to the SUMER oscillations that strongly damped (Wang et al. 2002, 2003; Wang 2011). However, the preflare-VLP is not significantly damping, so it could not be interpreted as the SUMER oscillation. On the other hand, the flare source region might accumulate magnetic energy by photospheric convection during the preflare phase, which can drive electric currents in the plasma loop (Tobias & Cattaneo 2013; Tan & Huang 2006; Tan et al. 2016). Therefore, the preflare-VLP is most likely to be explained as the LRC oscillation in the current-carrying plasma loop, which can modulate both thermal and nonthermal emissions (e.g., Tan et al. 2010, 2016; Li et al. 2016, 2020b). Previous studies (Zaitsev et al. 1998, 2000) suggested that the LRC oscillation period (P) could depend on the cross-sectional area (S), the plasma density (ρ), and the electric current (I), such as $P \approx (2.75 \times 10^4\, S\, \rho^{0.5})/I$ (see, Tan et al. 2016). The cross-sectional area could be estimated from the source region in Hα images, which is fitted with a elliptic function, as outlined by the yellow dashed line in Figs. 1b and c. This is based on the fact that the outer profiles of the source region hardly expand over time in the chromosphere (see Zhang et al. 2019), which can also be seen in the online video, anim.mp4. The elliptic area following a correction of the projection effect is about 1.2×10^{14} m^2. The typical value in the flaring coronal loop is referred to as the plasma density, that is, $\rho \sim 1.67 \times 10^{-11}$ kg m^{-3} (Bray et al. 1991; Tan et al. 2016; Tian et al. 2016). Considering a period of ~9.3 min, the electric current in the preflare phase is estimated to be roughly $I \approx 2.4 \times 10^{10}$ A. The estimated electric current here is lower than those taking place during solar flares, that is, as high as $\sim 10^{12}$ A (e.g., Canfield et al. 1993; Tan & Huang 2006). However, we should state that the preflare-VLP appears prior to the onset of a solar flare, which also agrees with previous findings in preflare phases (see, Tan et al. 2016), so this result is reasonable.

In this Letter, we first report a preflare-VLP in the Hα emission, which could be regarded as a precursor to an M1.1 circular-ribbon flare. It can be adequately explained by the LRC model. The time lag between Hα and SXR light curves suggests that the driven energy originates from photospheric convection in the low atmosphere before propagating to the middle (Hα) and high (SXR) atmospheres.

Acknowledgements. We acknowledge the anonymous referee for their inspiring and valuable comments. We thank the teams of NVST, GOES and SDO for their open data use policy. This study is supported by NSFC under grant 11973092, 11803008, 11790302, 11729301, the Youth Fund of Jiangsu No. BK20171108, as well as National Natural Science Foundation of China (U1731241), the Strategic Priority Research Program on Space Science, CAS, Grant No. XDA15052200 and XDA15320301. The Laboratory No. 2010DP173032. D.L. is also supported by the Specialized Research Fund for State Key Laboratories and the CAS Key Laboratory of Solar Activity (KLSA202003). S. Feng is supported by the Joint Fund of NSFC (U1931107) and the key Applied Basic Research program of the Yuanan Province (2018FA035).

References

Anfinogentov, S. A., Nakariakov, V. M., & Nisticò, G. 2015, A&A, 583, A136
Aschwanden, M. J., Benz, A. O., Dennis, B. R., et al. 1995, ApJ, 455, 347
Benz, A. O. 2017, Liv. Rev. Sol. Phys., 14, 2
Bray, R. J., Cram, L. E., Durrant, C., et al. 1991, Plasma Loops in the Solar Corona (Cambridge, UK: Cambridge University Press)
Canfield, R. C., de La Beaujardiere, J.-F., Fan, Y., et al. 1993, ApJ, 411, 362
Dennis, B. R., Tolbert, A. K., Inglis, A., et al. 2017, ApJ, 836, 84
Duckenfield, T. J., Goddard, C. R., Pascoe, D. J., et al. 2019, A&A, 632, A64
Hayes, L. A., Gallagher, P. T., Dennis, B. R., et al. 2019, ApJ, 875, 33
Inglis, A. R., Ireland, J., Dennis, B. R., et al. 2016, ApJ, 833, 284
Jess, D. B., Morton, R. J., Verth, G., et al. 2015, Space Sci. Rev., 190, 103
Karlický, M., Chen, B., Gary, D. E., et al. 2020, ApJ, 889, 72
Kliem, B., Karlický, M., & Benz, A. O. 2000, A&A, 360, 715
Kolotkov, D. Y., Nakariakov, V. M., Kupriyanova, E. G., et al. 2015, A&A, 574, A53
Kupriyanova, E., Kolotkov, D., Nakariakov, V., et al. 2020, Solar-Terr. Phys., 6, 3
Lemen, J. R., Title, A. M., Akin, D. J., et al. 2012, Sol. Phys., 275, 17
Li, L. P., Zhang, J., Su, J. T., et al. 2016, ApJ, 829, L33
Li, D., Zhang, Q. M., Huang, Y., et al. 2017, A&A, 597, L4
Li, D., Li, Y., Su, W., et al. 2018, ApJ, 854, 26
Li, D., Kolotkov, D. Y., Nakariakov, V. M., et al. 2020a, ApJ, 888, 53
Li, D., Li, Y., Lu, L., et al. 2020b, ApJ, 893, L17
Li, D., Lu, L., Ning, Z., et al. 2020c, ApJ, 893, 7
Liang, B., Meng, Y., Feng, S., et al. 2020, Ap&SS, 365, 40
Liu, Z., Xu, J., Gu, B.-Z., et al. 2014, Res. Astron. Astrophys., 14, 705
McLaughlin, J. A., Nakariakov, V. M., Dominique, M., et al. 2018, Space Sci. Rev., 214, 45
Nakariakov, V. M., Ofman, L., Deluca, E. E., et al. 1999, Science, 285, 862
Nakariakov, V. M., Foullon, C., Myagkova, I. N., et al. 2010, ApJ, 708, L47
Nakariakov, V. M., Kolotkov, D. Y., Kupriyanova, E. G., et al. 2019a, Plasma Phys. Control. Fusion, 61, 014024
Nakariakov, V. M., Kosak, M. K., Kolotkov, D. Y., et al. 2019b, ApJ, 874, L1
Ning, Z. 2014, Sol. Phys., 289, 1239
Ning, Z. 2017, Sol. Phys., 292, 11
Ning, Z., Ding, M. D., Wu, H. A., et al. 2005, A&A, 437, 691
Parks, G. K., & Winckler, J. R. 1969, ApJ, 155, L117
Pugh, C. E., Broomhall, A.-M., & Nakariakov, V. M. 2019, A&A, 624, A65
Shen, Y. D., Liu, Y., Su, J. T., et al. 2013, Sol. Phys., 288, 585
Shen, Y., Chen, P. F., Liu, Y. D., et al. 2019, ApJ, 873, 22
Srivastava, A. K., Zaqarashvili, T. V., Uddin, W., et al. 2008, MNRAS, 388, 1899
Su, J. T., Ji, K. F., Banerjee, D., et al. 2016, ApJ, 816, 30
Tan, B. L., & Huang, G.-L. 2006, A&A, 453, 321
Tan, B., Yan, Y., Tan, C., et al. 2007, ApJ, 671, 964
Tan, B., Zhang, Y., Tan, C., et al. 2010, ApJ, 723, 25
Tan, B., Yu, Z., Huang, J., et al. 2016, ApJ, 833, 206
Tian, H., McIntosh, S. W., Wang, T., et al. 2012, ApJ, 759, 144
Tian, H., Young, P. R., Reeves, K. K., et al. 2016, ApJ, 823, L16
Thurgood, J. O., Pontin, D. I., & McLaughlin, J. A. 2017, ApJ, 844, 2
Tobias, S. M., & Cattaneo, F. 2013, Nature, 497, 463
Tubbs, R. N. 2004, The Observatory, 124, 159
Van Doorsselaere, T., Kupriyanova, E. G., & Yuan, D. 2016, Sol. Phys., 291, 3143
Wang, T. 2011, Space Sci. Rev., 158, 397
Wang, T., Solanki, S. K., Curdt, W., et al. 2002, ApJ, 574, L101
Wang, T. J., Solanki, S. K., Curdt, W., et al. 2003, A&A, 406, 1105
Wang, T., Ofman, L., Sun, X., et al. 2015, ApJ, 811, L13
Woods, T. N., Eparvier, F. G., Hock, R., et al. 2012, Sol. Phys., 275, 115
Xiang, Y. Y., Liu, Z., & Jin, Z. Y. 2016, New Astron., 49, 8
Xu, Z., Jin, Z. Y., Xu, F. Y., et al. 2014, Nature of Prominences and Their Role in Space Weather, 117
Yang, S., & Xiang, Y. 2016, ApJ, 819, L24
Yu, S., & Chen, B. 2019, ApJ, 872, 71
Yuan, D., Feng, S., Li, D., et al. 2019, ApJ, 886, L25
Zaitsev, V. V., Stepanov, A. V., Urpo, S., et al. 1998, A&A, 337, 887
Zaitsev, V. V., Urpo, S., & Stepanov, A. V. 2000, A&A, 357, 1105
Zhang, Q. M., & Zheng, R. S. 2020, A&A, 633, A142
Zhang, Q. M., Su, Y. N., & Ji, H. S. 2017, A&A, 598, A3
Zhang, Q. M., Cheng, J. X., Feng, L., et al. 2019, ApJ, 883, 124
Zhou, G. P., Zhang, J., & Wang, J. X. 2016, ApJ, 823, L19